# We are IntechOpen,
# the world's leading publisher of
# Open Access books
# Built by scientists, for scientists

## 4,800
Open access books available

## 122,000
International authors and editors

## 135M
Downloads

Our authors are among the

## 154
Countries delivered to

## TOP 1%
most cited scientists

## 12.2%
Contributors from top 500 universities

CLARIVATE ANALYTICS
**BOOK CITATION INDEX**
INDEXED

**WEB OF SCIENCE**™

Selection of our books indexed in the Book Citation Index
in Web of Science™ Core Collection (BKCI)

## Interested in publishing with us?
## Contact book.department@intechopen.com

# Compost Process and Organic Fertilizers Application in China

Guanghui Yu, Wei Ran and Qirong Shen

Additional information is available at the end of the chapter

## Abstract

Composting is an inexpensive and sustainable treatment for solid wastes. The composting industry has been growing rapidly because of a boom in the animal industry in China over the past decades. In this chapter, we introduce composting process and status in China, especially in Jiangsu Province. Meanwhile, the developed novel spectroscopy techniques are also introduced, which are more suitable for assessment of compost maturity than the conventional techniques in view of ease of sample preparation, rapid spectrum acquisition, and nondestructive nature of the analysis. These novel spectroscopy techniques include near-infrared reflectance spectroscopy (NIRS)—partial least squares (PLS) analysis and fluorescence excitation–emission matrix (EEM) spectroscopy—parallel factor (PARAFAC) analysis. In addition, organic fertilizer amendments can not only improve soil fertility but also offset chemical fertilizers' nanoscale changes. Emerging cutting-edge technologies of synchrotron-based X-ray absorption fine structure (XAFS) spectroscopy and nanoscale secondary ion mass spectrometry (NanoSIMS) were used to identify the composition of organic carbon and minerals and their correlations, respectively. Recently, investigators have shown that organic fertilizer amendments could enhance the production of highly reactive minerals, for example, allophane, imogolite, and ferrihydrite, which further benefit for soil carbon storage and soil fertility improvement.

**Keywords:** compost process, compost maturity, China, solid waste treatment, soil fertility, spectroscopy techniques, nanominerals, short-range ordered minerals, soil carbon storage

## 1. Introduction

Composting is an inexpensive, efficient, and sustainable treatment for solid wastes. In China, the composting industry has been growing rapidly, owing to a boom in the animal industry over the past decades. Because an immature compost applied to soil results in seed germination inhibition, root destruction, and a decrease in the $O_2$ concentration and redox potential [1, 2], assessing organic fertilizer maturity is critical. By the way, a main difference between common composts and commercial organic fertilizers is the complexity and unpredictability of the raw materials of the latter.

In recent decades, livestock numbers have increased dramatically in China. The quantity of manure generated by China's livestock has increased significantly as a result of the rapid increases in livestock numbers. The quantity increased by at least fourfold between 1980 and 2005, to an annual estimated total of 3060 million tons (Mt, fresh weight of manure) in 2005. [3] It was estimated that manure generation in 2010 was ca. 2800 Mt (fresh weight). [3] In addition, organic fertilizer amendment has been shown to be an effective way of increasing soil organic matter (SOM) content and reducing environmental pollution. However, the mechanism of storage of SOM remains largely unknown. Recently, some investigators have shown that organic fertilizer amendments could enhance the production of highly reactive short-range ordered (SRO) minerals, which further benefit for SOM storage and soil fertility improvement. [4–6]

In this chapter, compost process and status, novel spectroscopy techniques in assessing compost maturity, and improvement of soil fertility by organic fertilizer amendments in China are introduced.

## 2. Compost process and status in China

Traditionally, farmers in China were mainly depending on organic fertilizers, for example, animal manures and agricultural residuals. In 1950s, farmers also began to apply some of chemical fertilizers (**Figure 1**). In 1980s, the application of chemical fertilizers and organic fertilizers had a very similar percentage. However, the application of chemical fertilizers in 2010 was over 90%. As a result, soil acidification is a major problem in soils of intensive Chinese agricultural systems. Two nationwide surveys showed that soil pH declined significantly ($P < 0.001$) from the 1980s to the 2000s in the major Chinese crop-production areas. [7] Therefore, the replacement of chemical fertilizers by organic fertilizers in a certain percentage is urgent.

During the last decade's development of composting in China, numerous large-scale animal farms with more than 10,000 pigs or 5000 cattle have been established. As a result, a large amount of animal manure is produced, which is a major pollutant if untreated [8]. On the other hand, this is also a perfect resource of organic fertilizers. For example, more than 100 factories produce over 5000 tons of commercial organic fertilizers each year in Jiangsu Province, China (**Figure 2**). Correspondingly, the Jiangsu government now subsidizes the composting factories
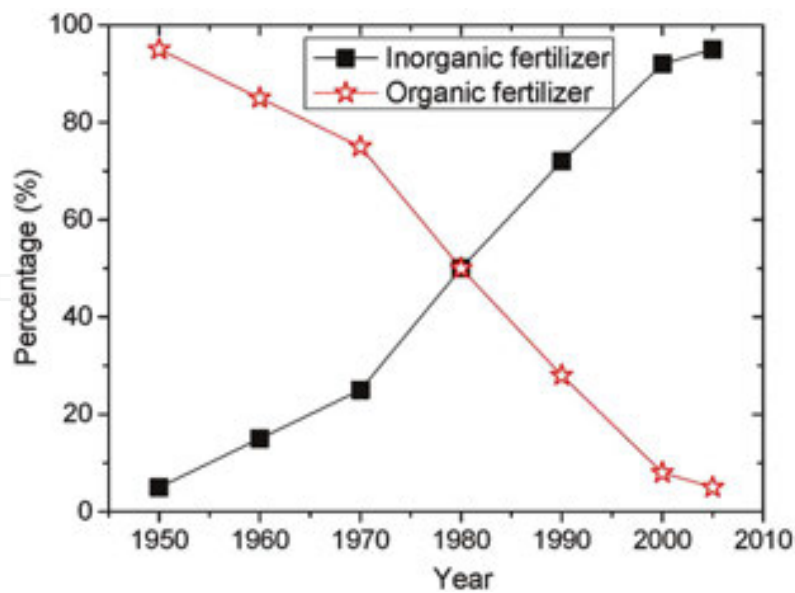
**Figure 1.** Percentage of fertilizers used in China from 1950 to 2005.

with 200 RMB per ton. As a result, the price of commercial organic fertilizers has decreased from 550 to 350 RMB. Therefore, the farmers are pleased to replace chemical fertilizers with commercial organic fertilizers. Presently, the total amount of commercial organic fertilizers produced by subsidized composting facilities is more than 2 million tons per year in Jiangsu Province, China (**Figure 2**). Thereof, the government of Jiangsu Province plays a critical role in promoting the production and application of organic fertilizers by the farmers.



**Figure 2.** Summary of factory locations to produce commercial organic fertilizers in Jiangsu Province, China.
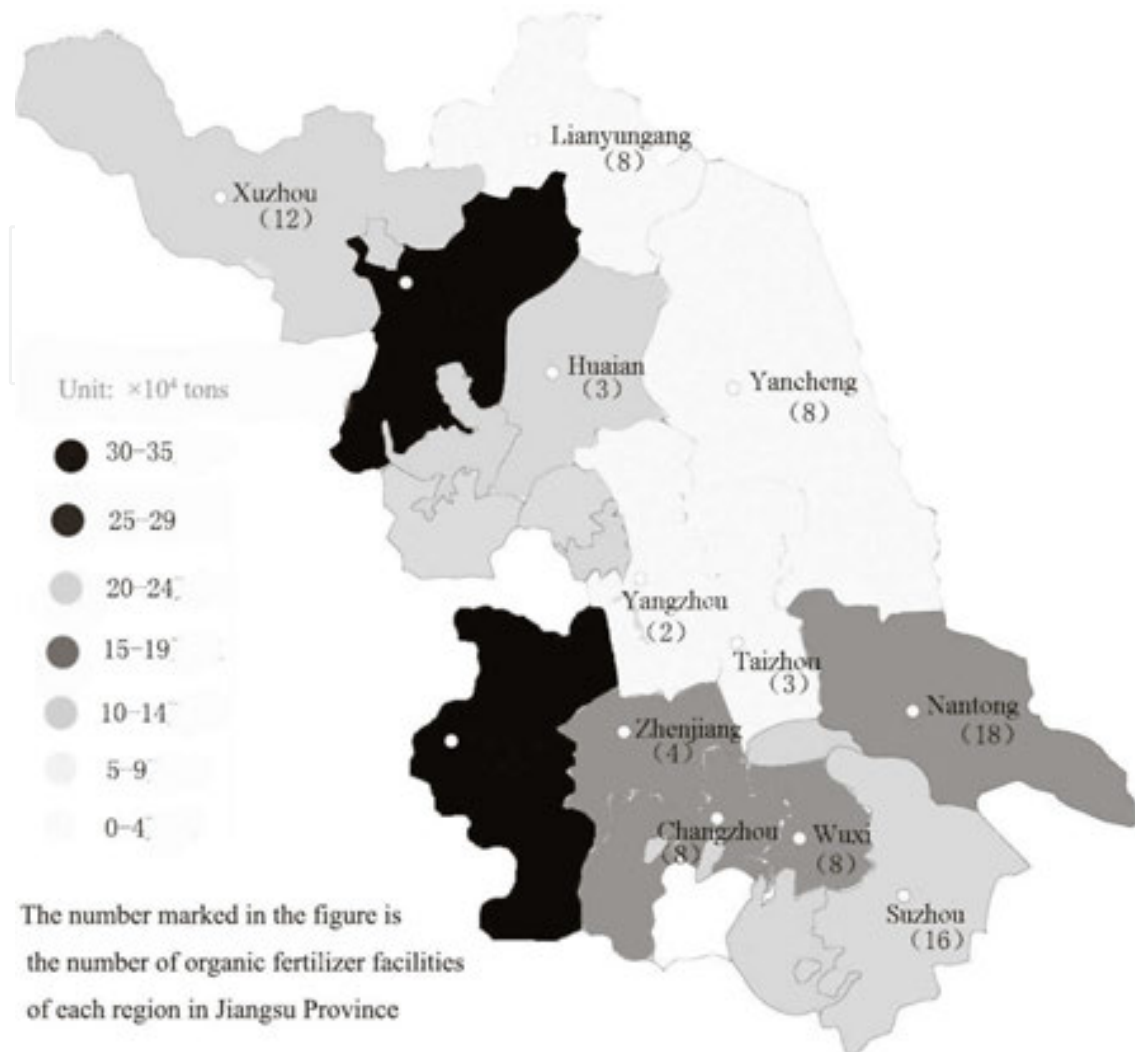
**Figure 3.** Trough composting system (a) and windrow composting system (b) in China.

In China, trough composting system and windrow composting system are the main compost-ing processes, with windrow composting system being more popular in Jiangsu Province (**Figure 3**). Windrow composting consists of placing the mixture of raw materials in long narrow piles that are agitated or turned on a regular basis. The turning mixes the materials during composting and enhances passive aeration. Generally, the heights of windrows are in a range of 90 to 180 cm. Correspondingly, the width of them varies in a range of 100 to 300 cm. In general, the size, shape, and spacing of the windrows are determined by the turning equipment. During aeration, the rate of air exchange depends on the porosity of the windrow. Therefore, the size of a windrow is determined by its porosity.

## 3. Assessment of compost maturity by spectroscopy techniques

Various parameters are commonly used to evaluate compost quality. [9] In general, these parameters include germination index (GI), water-soluble organic carbon (WSOC), water-

soluble organic nitrogen (WSON), pH, electrical conductivity (EC), moisture, and total organic matter (TOM) content. It is accepted that any sole parameter cannot determine compost maturity, which must be assessed by a combination of different physical, chemical, and biological properties (**Table 1**). However, all these approaches are expensive or time-consuming when a large number of samples are involved. [1,10] It is reported that spectroscopy techniques have many advantages over traditional chemical analyses, such as its ease of sample preparation, rapid spectrum acquisition, nondestructive analysis, and portability. [11]

| Physical | Odor, color, temperature, particle size and inert materials | |
|---|---|---|
| Chemical | Carbon and nitrogen analyses | C/N ratio in solid and water extract |
| | Cation exchange capacity | CEC, CEC/Total organic-C ratio, etc |
| | Water-soluble extract | pH, EC, organic-C, ions, etc |
| | Mineral nitrogen | $NH_4$-N content, $NH_4$-N/$NO_3$-N ratio |
| | Pollutants | Heavy metals and organics |
| | Organic matter quality | Organic composition: lignin, complex carbohydrates, lipids, sugars, etc. |
| | Humification | Humification indices and humic-like substances characterization: elemental and functional group analyses, molecular weight distribution, E4/E6 ratio, pyrolysis GC-MS, spectroscopic analyses (NMR, FTIR, Fluorescence, Raman, etc.) |
| Biological | Microbial activity indicators | Respiration ($O_2$ uptake/consumption, self-heating test, biodegradable constituents) |
| | | Enzyme activity (cellulase, phosphatases, dehydrogenases, proteases, etc) |
| | | ATP content |
| | | Nitrogen mineralization-immobilization potential, nitrification, etc. |
| | | Microbial biomass |
| | Phytotoxicity | Germination and plant growth tests |
| | Others | Viable weed seed, pathogen, and ecotoxicity tests |

**Table 1.** Current criteria evaluated in the literature to characterize compost quality [9]

Near-infrared reflectance spectroscopy (NIRS) has been shown to rapidly (within 1 min) assess compost quality. [12–14] However, it is unclear whether NIRS can also be applied to rapidly determine the quality of commercial organic fertilizers, owing to the complexity and unpredictability of the raw materials of the commercial products. **Figure 4** shows a distinct appearance of commercial organic fertilizers with composting samples. A total of 104 commercial

organic fertilizers were collected from full-scale compost factories in Jiangsu Province, China. These factories treat organic matter from animal manure and other agricultural organic residues. These factories produce approximately 5000–150,000 tons of commercial organic fertilizers per year.
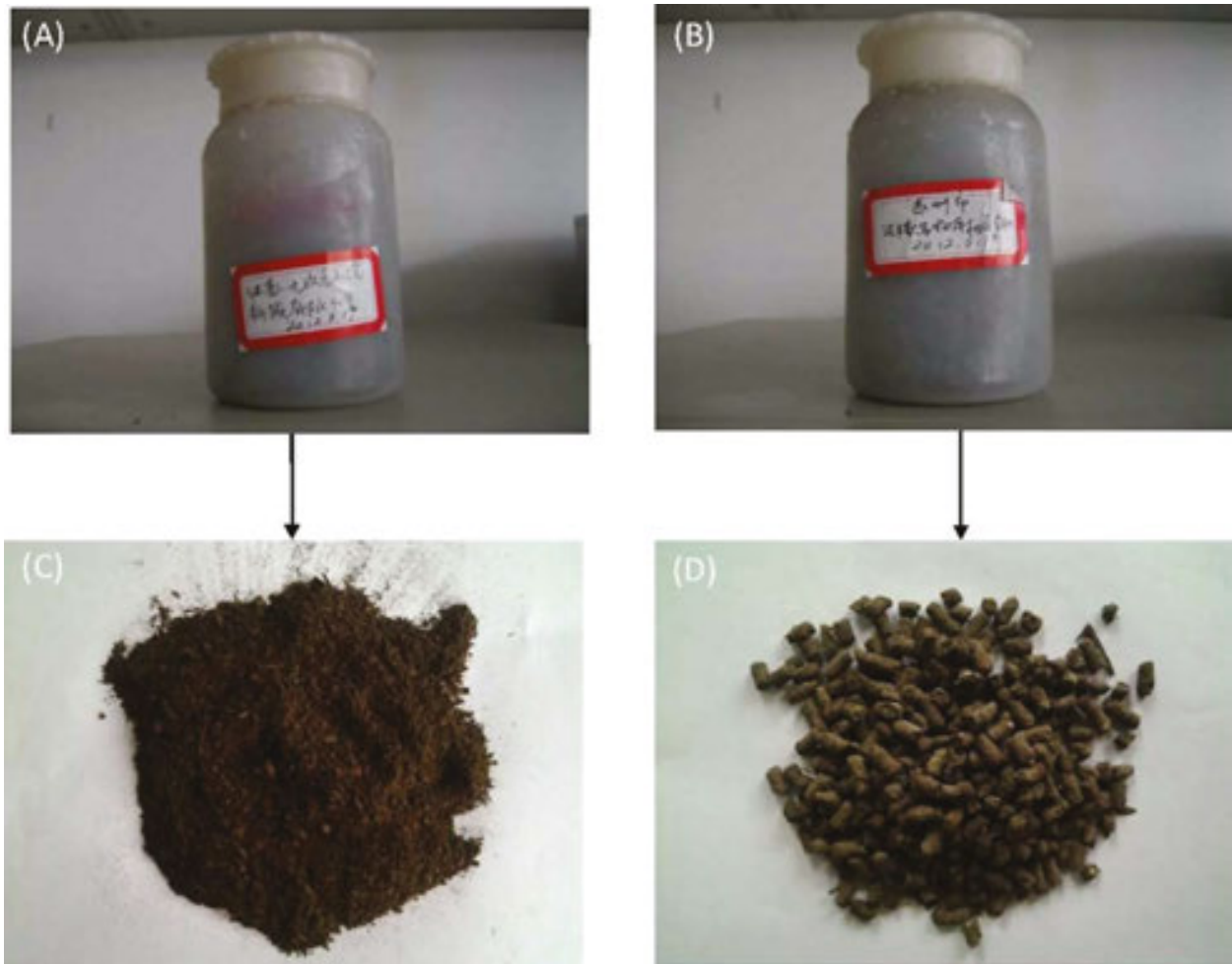


**Figure 4.** Typical commercial organic fertilizers, including powered (A, C) and granular (B, D) fertilizers. These photos suggest that the commercial organic fertilizers are more even than samples from the composting process.

We can see that all the NIR spectra collected from commercial organic fertilizers in Jiangsu Province, China (**Figure 5**) were divided into two groups of signals with different slopes under 1400 nm: one group has an increased curvature with a significant absorbance peak at a wavelength of approximately 1420 nm, while another is more flat and has only a small absorption at this position. This is because the second significant spectral peak is mainly at approximately 1950 nm (**Figure 5**). The band at 1420 nm is associated with the O–H and aliphatic C–H, while that at 1950 nm is assigned to the amide N–H and O–H. Because the NIR spectrum contains all strength information of the chemical bond, chemical composition, electronegativity, etc, the absorption peaks are heavily overlapped. In addition, other interference information, such as scattering, diffusion, special reflection, refractive index, and

reflected light polarization, also has an important influence on the NIR spectrum. Thus, the quantitative predictions are difficult directly through NIR spectra alone.
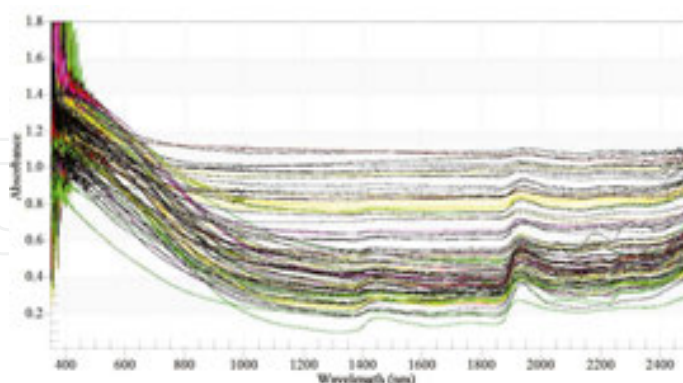


**Figure 5.** Spectra of NIR of a total of 104 commercial organic fertilizers. [10]

Multivariate analyses are required to discern the spectral characteristics of commercial organic fertilizers with the support of chemometric methods, for example, partial least squares (PLS) analysis in this study. The results of the NIRS calibration and validation for the quality indices of commercial organic fertilizers are listed in **Table 2** and Figures 6 and 7. The NIR calibrations allowed accurate predictions of WSON, TOM, pH, and GI ($R^2 = 0.73$–$0.93$ and RPD = 1.47–2.96). However, the results were less accurate for moisture ($R^2 = 0.91$, $r^2 = 0.79$, RPD = 2.22), TN ($R^2 = 0.98$, $r^2 = 0.80$, RPD = 2.25), and EC ($R^2 = 0.99$, $r^2 = 0.74$, RPD = 2.27). In addition, the WSOC had the worst prediction ($R^2 = 0.88$, $r^2 = 0.76$, RPD = 2.10). Therefore, predictions were moderately successful for TOM, TN, WSON, pH, EC, GI, and moisture, but failed for WSOC.
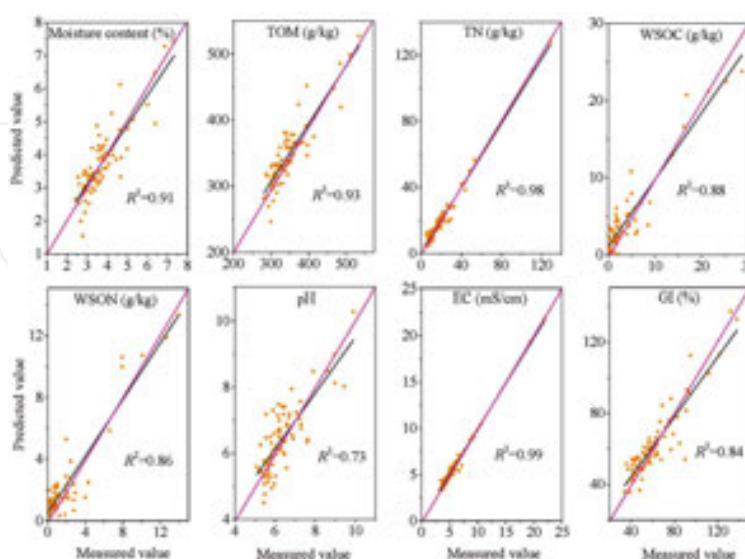


**Figure 6.** The measured and predicted values of the quality indices of commercial organic fertilizers in the calibration data set. [10] The best fit is shown by red line.
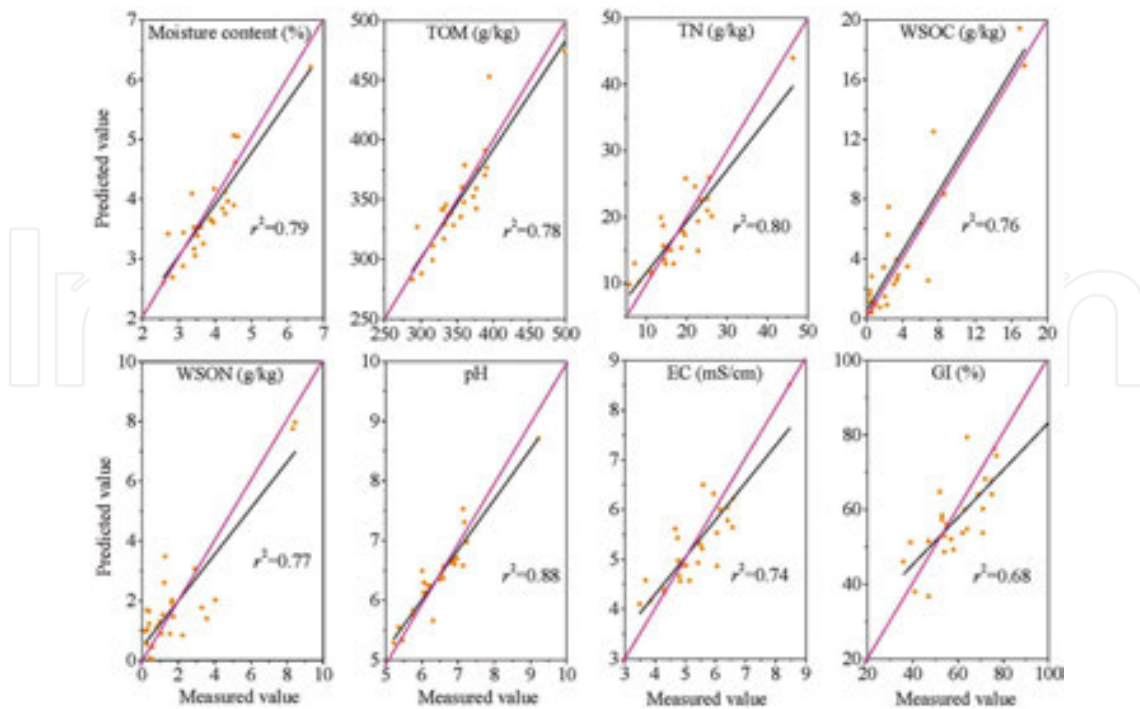
**Figure 7.** The measured and predicted values of the quality indices of commercial organic fertilizers in the prediction data set. [10] The best fit is shown by red line.

| Parameters | Calibration set | | | Validation set | | | | |
|---|---|---|---|---|---|---|---|---|
| | PC | $R^2$ | RMSECV | $r^2$ | RMSEP | RPD | Bias | Slope |
| Moisture content (%) | 19 | 0.94 | 0.23 | 0.67 | 0.36 | 2.27 | −0.03 | 0.76 |
| TOM (g/kg) | 12 | 0.85 | 17.69 | 0.69 | 24.76 | 1.71 | −9.03 | 0.72 |
| TN (g/kg) | 17 | 0.98 | 3.08 | 0.80 | 3.63 | 2.25 | −0.29 | 0.77 |
| WSOC (g/kg) | 7 | 0.85 | 3.82 | 0.55 | 3.21 | 1.43 | 0.06 | 0.69 |
| WSON (g/kg) | 8 | 0.86 | 1.81 | 0.77 | 1.60 | 1.47 | 0.05 | 0.74 |
| pH | 9 | 0.86 | 0.36 | 0.75 | 0.41 | 1.96 | −0.10 | 0.73 |
| EC (mS/cm) | 17 | 0.99 | 0.46 | 0.74 | 0.54 | 2.27 | −0.04 | 0.78 |
| GI (%) | 18 | 0.84 | 4.81 | 0.68 | 9.52 | 1.73 | −2.68 | 0.63 |

TOM, total organic matter; TN, total nitrogen; WSOC, water-soluble organic carbon; WSON, water-soluble organic nitrogen; EC, electrical conductivity; GI, germination index; PC, number of principal components; $R^2$, the coefficient of determination for the calibration set; RMSECV, the root mean squared error in cross-validation; $r^2$, the coefficient of determination for the validation set; RMSEP, room mean squared error of prediction; RPD, the ratio of the standard deviation in the validation set over the room mean squared error of prediction.

**Table 2.** NIRS calibration and validation results for quality indices of commercial organic fertilizers [10]

Similar to NIRS, fluorescence excitation–emission matrix (EEM) spectroscopy is extensively utilized to detect protein-like, fulvic-acid-like, and humic-acid-like substances. These materials

are directly proportional to fluorescence intensity at low concentrations and thus are applied to assess compost maturity [15]. Fluorescence spectroscopy has been widely used as a tool to assess compost maturity, owing to high instrumental sensitivity. [16] However, analysis of fluorescence EEM has generally been limited to visual identification of peaks or development of ratios of fluorescence intensities in different regions of the spectrum. These techniques lack the ability to capture the heterogeneity of samples. It has been reported that as opposed to individual main peak positions analysis, analyzing the full fluorescence EEMs can provide much information. [17] Additionally, the composition complexity of WEOM in compost samples often results in the overlapped fluorophores in the EEM spectra. As a result, the EEM spectra are difficult to interpret.

Recent work has demonstrated that parallel factor (PARAFAC) analysis can be used to decompose full fluorescence EEMs into different independent groups of fluorescent components. [18] Therefore, EEM-PARAFAC analysis is able to assess compost maturity and also to be a potential monitoring tool for rapidly characterizing compost maturity. For this purpose, 62 full-scale compost facilities in nine Provinces of China, yielding compost from animal manures and other industrial organic residues of different maturities, were selected. Then, these compost samples were used to extract water-soluble OM (WEOM) and characterized by fluorescence EEM spectra. EEM-PARAFAC analysis was then conducted for assessment of compost maturity.

**Figure 8** shows the typical fluorescence EEM contours of WEOM. The EEM contours of WEOM between mature and immature composts were obviously distinct. Specifically, the former had only two peaks (A and B), while the latter exhibited four peaks (A, B, C, and D) (**Figure 8**).
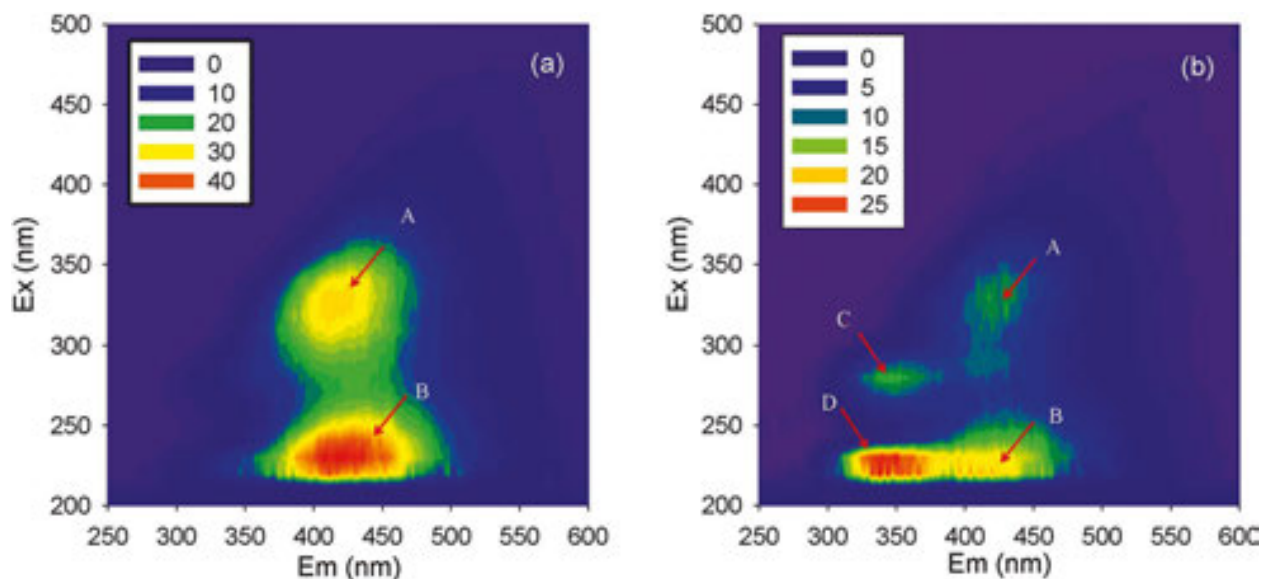


**Figure 8.** Typical EEM contours of mature (a) and immature (b) composts, [1] normalized to 1 mg DOC/L. Note: The arrows refer to the location of peaks. Specifically, two peaks at Ex/Em of 230/420 (B) and 330/420 (A) were presented in mature composts, whereas four peaks at Ex/Em of 220/340 (D), 280/340 (C), 220/410 (B), and 330/410 (A) were detected in the immature composts.

The fluorescence EEM contours were interpreted using the protocol of the previous literature. [17] The typical mature compost contained humic-acid-like substances (i.e., Peak A: Ex/Em = 330/420) and fulvic-acid-like substances (i.e., Peak B: Ex/Em = 230/420) in the WEOM of compost. The typical immature WEOM of compost, however, in addition to containing humic acid–like substances (Peak A) and fulvic acid–like substances (Peak B), also contained tryptophan-like substances (i.e., Peak D: Ex/Em = 220/340) and a few soluble microbial by-product–like (SMP) substances (i.e., Peak C: Ex/Em = 280/340). The above results were consistent with those of Marhuenda-Egea et al. in that the composting process was a degradation of the original tyrosine-like and tryptophan-like materials and an increase in the humic-like and fulvic-like materials. [19] As composting time increased, molecular heterogeneity decreased, while aromatic polycondensation, level of conjugated chromophores, and humification degree increased, as shown by fluorescence EEM spectra. [20] Therefore, fluorescence EEMs of the WEOM from composts had the potential to be used as a monitoring tool for rapidly assessing the maturity of compost.

Preprocessing of the fluorescence EEMs is essential to acquire a correct component number before PARAFAC analysis. After removing the Rayleigh and Raman scatters, the sum of squared residuals in the excitation (Ex) and emission (Em) directions for three different models are plotted in **Figure 9a**. By comparing the two-, three-, and four-component models, it is clear that the step from the two- to three-component model showed great improvement of fit, whereas the step from the three- to four-component model offered only some enhancement of fit. This result suggests that three components are adequate for this data. Split-half analysis further validated the close-to-perfect correspondence between the Ex and Em loadings for the three components, using the four independent random halves (**Figure 9b**). Thus, three components were suitable for all of the examined samples. The EEM contours are shown in
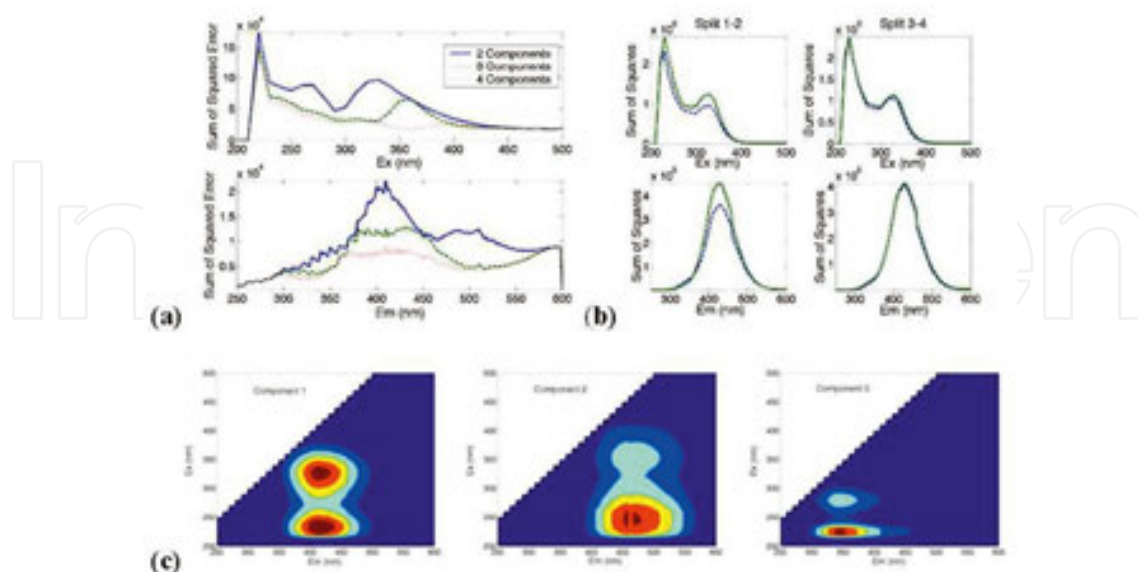


**Figure 9.** PARAFAC analysis of 60 compost samples. (a) Sum of squared error for determining the component numbers. (b) Split-half analysis for model validation. (c) EEM contours of identified components. [1]

**Figure 9c**. All the EEMs in this study could be decomposed into a three-component model by PARAFAC analysis, with component 1 [Ex/Em = (230, 330)/410], component 2 [Ex/Em = (250, 350)/450], and component 3 [Ex/Em = (220, 280)/340]. The three components belonged to humic-like, fulvic-like, and protein-like substances, respectively.

Clearly, component 1 was humic fluorophores derived from both terrestrial-like and marine-like, and component 2 was terrestrial-like humic fluorophores. In contrast, component 3 was a tryptophan-like substance. In addition, all the components displayed the same Em wavelength at different Ex wavelengths, possibly attributable to the rapid internal conversion of excited electrons to the lowest vibration level of the first excited state. **Table 3** shows that component 1 was strongly correlated with components 2 and 3, whereas components 2 and 3 had no significant correlation, indicating that component 1 has a common source with components 2 and 3, but components 2 and 3 do not have the same source.

|  | Component 1 | Component 2 | Component 3 | TOC | C/N | TOC/TN | OM | MI | GI | OUR | CER |
|---|---|---|---|---|---|---|---|---|---|---|---|
| Component 1 | 1 | 0.40[b] | 0.89[b] | 0.35[b] | −0.05 | −0.15 | 0.40[b] | −0.22 | −0.39[b] | 0.40[b] | 0.43[c] |
| Component 2 |  | 1 | 0.18 | 0.57[c] | −.16 | −0.11 | 0.20 | −0.11 | −0.22 | 0.30[a] | 0.37[b] |
| Component 3 |  |  | 1 | 0.51[c] | 0.04 | −0.04 | 0.54[c] | −0.29 | −0.37[b] | 0.40[b] | 0.39[b] |
| TOC |  |  |  | 1 | −0.11 | 0.07 | 0.53[c] | −0.32[a] | −0.38[b] | 0.35[b] | 0.33[a] |
| C/N |  |  |  |  | 1 | 0.13 | 0.25 | −0.15 | 0.38[b] | −0.08 | −0.04 |
| TOC/TN |  |  |  |  |  | 1 | −0.06 | 0.19 | 0.31[a] | 0.13 | 0.04 |
| OM |  |  |  |  |  |  | 1 | −0.76[b] | −0.06 | 0.11 | 0.06 |
| MI |  |  |  |  |  |  |  | 1 | 0.18 | −0.06 | −0.03 |
| GI |  |  |  |  |  |  |  |  | 1 | −0.27[a] | −0.29[a] |
| OUR |  |  |  |  |  |  |  |  |  | 1 | 0.84[c] |
| CER |  |  |  |  |  |  |  |  |  |  | 1 |

[a] Correlation is significant at the 0.05 level (two-tailed).
[b] Correlation is significant at the 0.01 level (two-tailed).
[c] Correlation is significant at the 0.001 level (two-tailed). OM, organic matter; MI, mineralization index; GI, germination index; OUR, oxygen uptake rate; CER, $CO_2$ evolution rate.

**Table 3.** Pearson correlation between log (scores) of PARAFAC components and selected stability indices ($n = 60$) [1]

In addition, components 1 and 3 had a strong correlation ($R > 0.35$, $p < 0.01$) with TOC, OM, CER, GI, and OUR. But component 2 was only significantly ($R > 0.37$, $p < 0.01$) correlated with TOC and CER, and weakly ($R = 0.30$, $p < 0.05$) correlated with OUR (**Table 4**). Therefore, components 1 and 3 are more suitable to assess compost maturity than component 2. Furthermore, the regression equations in **Table 4** indicated that the composts could be identified as mature when the log scores of components 1 and 3 were higher than $3.69 \pm 0.06$ and $3.49 \pm 0.09$, respectively.

| | Indices (x) | Regression equation | Maturity value in the literature [9] | Calculated log (scores) of components |
|---|---|---|---|---|
| Component 1 (y) | TOC | $y = 3.7 + 7.5 \times 10^{-3}x$ | 10 mg/g-DM | 3.78 |
| | OM | $y = 3.3 + 1.1 \times 10^{-2}x$ | 30% | 3.63 |
| | GI | $y = 4.0 - 6.8 \times 10^{-3}x$ | 50% | 3.66 |
| | OUR | $y = 3.7 + 3.6 \times 10^{-3}x$ | 10 mg $O_2$/g-OM/d | 3.74 |
| | CER | $y = 3.6 + 8.9 \times 10^{-3}x$ | 4 mg C-$CO_2$/g-OM/d | 3.64 |
| Component 3 (y) | TOC | $y = 3.5 + 1.2 \times 10^{-2}x$ | 10 mg/g-DM | 3.62 |
| | OM | $y = 2.9 + 1.6 \times 10^{-2}x$ | 30% | 3.38 |
| | GI | $y = 3.8 - 6.8 \times 10^{-3}x$ | 50% | 3.46 |
| | OUR | $y = 3.5 + 3.9 \times 10^{-3}x$ | 10 mg $O_2$/g-OM/d | 3.54 |
| | CER | $y = 3.4 + 8.8 \times 10^{-3}x$ | 4 mg C-$CO_2$/g-OM/d | 3.44 |

TOC, total organic matter; OM, organic matter; GI, germination index; OUR, oxygen uptake rate; CER, $CO_2$ evolution rate.

**Table 4.** Calculated log (scores) of components from regression equations ($n = 60$) [1]

Some investigators have shown great interest in the assessment of compost maturity using fluorescence intensity. Our results demonstrate that log scores of components 1 and 3, identified by the DOMFluor–PARAFAC approach, can be applied to assess the maturity of composts which cover a large range of waste sources. This is attributable to the fact that the full fluorescence spectroscopy analysis provides a basis for capturing subtle changes in the fluorescence spectra. In summary, the assessment of compost maturity by the DOMFluor–PARAFAC approach is not wastesource–specific.

# 4. Impact of application of organic fertilizers on the soil properties

It is well known that organic fertilizer amendments can enhance soil fertility, increase soil aggregation, and increase soil pH (e.g., acidic soils). [21–23] For example, long-term (over 20 years) organic fertilization or organic plus inorganic fertilization could markedly improve soil organic carbon (SOC) content when compared to no fertilization (Control) and chemical fertilization (NPK) (**Figure 10**). Using Nano-CT, the structure of long-term fertilized soils at the Jinxian Experiment station was examined (**Table 5**). It was found that long-term organic amendments improved soil aggregation by decreasing the number of pores, pore throats, and paths between adjacent nodal pores in soil aggregates (**Table 5**). [24]
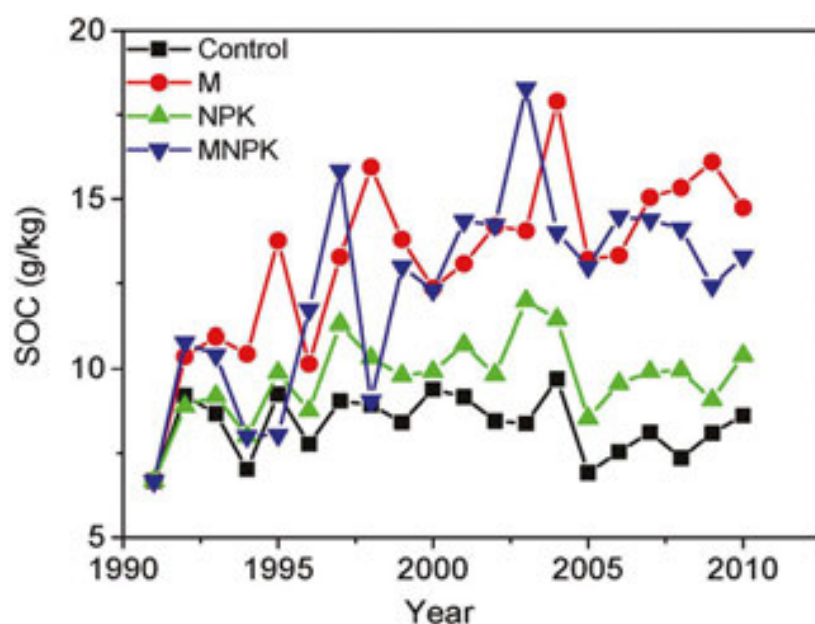
**Figure 10.** Dynamics of soil organic carbon (SOC) with fertilization time at the Qiyang long-term fertilization experiment station.

| Pore properties | No fertilizer input | Organic plus chemical amendments | Chemical fertilizer input |
|---|---|---|---|
| Porosity (%) | 14.2 (1.7)a | 13.2 (1.3)a | 14.9 (2.3)a |
| Macroporosity (>500 μm) (%) | 3.4 (0.6)b | 6.7 (0.4)a | 3.6 (0.7)b |
| Mesoporosity (≤500 μm) (%) | 10.8 (1.1)a | 6.5 (0.4)b | 11.3 (1.6)a |
| Total no. of pores | 3308 (313)a | 2288 (502)b | 2695 (267)ab |
| No. of interior pores | 2676 (407)a | 1881 (352)b | 2189 (268)ab |
| No. of boundary pores | 632 (250)a | 404 (68)b | 505 (87)ab |
| Fraction interior pores (%) | 55.2 (5.2)a | 33.0 (7.2)b | 29.3 (2.9)b |
| Fraction boundary pores (%) | 44.8 (5.2)b | 67.0 (7.2)a | 70.7 (2.9)a |
| Total no. of throats | 3709 (704)a | 1526 (257)b | 2698 (432)ab |
| Mean area of throats ($\mu m^2$) | 2913 (337)a | 3148 (342)a | 3803 (469)a |
| Specific surface area ($\mu m^{-1}$) | 8.50 (1.50)a | 5.80 (2.62)a | 7.80 (1.81)a |
| Total no. of paths | 6218 (1028)a | 3277 (988)b | 4927 (1346)a |
| Average length of paths (μm) | 158 (14)a | 175 (19)a | 169 (27)a |

Values in parentheses represent the standard deviation of the mean. Different letters following values between different fertilization treatments indicate significant differences at $P < 0.05$ (LSD). The soil at the Jinxian Experiment station is red soil.

**Table 5.** Summary of soil microstructure properties from three contrasting fertilization treatments at the Jinxian Experiment station, Jiangxi Province, China [24]

However, very few studies are conducted on how organic fertilizer amendments affect the morphology and coordinate state of nanominerals or organomineral associations in soil. High-resolution transmission electron microscopy (HRTEM) coupled to selected area electron diffraction (SAED) technique could be a promising tool to observe the morphology/appearance of nanominerals in soil dissolved organic matter (DOM). Under three fertilization treatments at the Qiyang Experiment station, HRTEM observation showed two regions (i.e., black and gray regions) of soil DOM with distinctive percentage presented under Control (no fertilization), NPK (chemical nitrogen, phosphorus, and potassium fertilization), and NPKM (NPK plus manure fertilization) at the 22 years' long-term fertilization site (**Figures 11–13**). The electron diffraction patterns indicated that the obtained nanominerals in the black and gray regions had a determinate crystalline and amorphous pattern, respectively. Elemental maps further confirmed that crystalline nanominerals were dominated by Fe and O, while amorphous nanominerals were mainly composed of Al, Si, and O (**Figures 11–13**). These results showed that after 22 years' fertilization, crystalline nanominerals were predominant under NPK, while amorphous nanominerals under both the Control and NPKM.
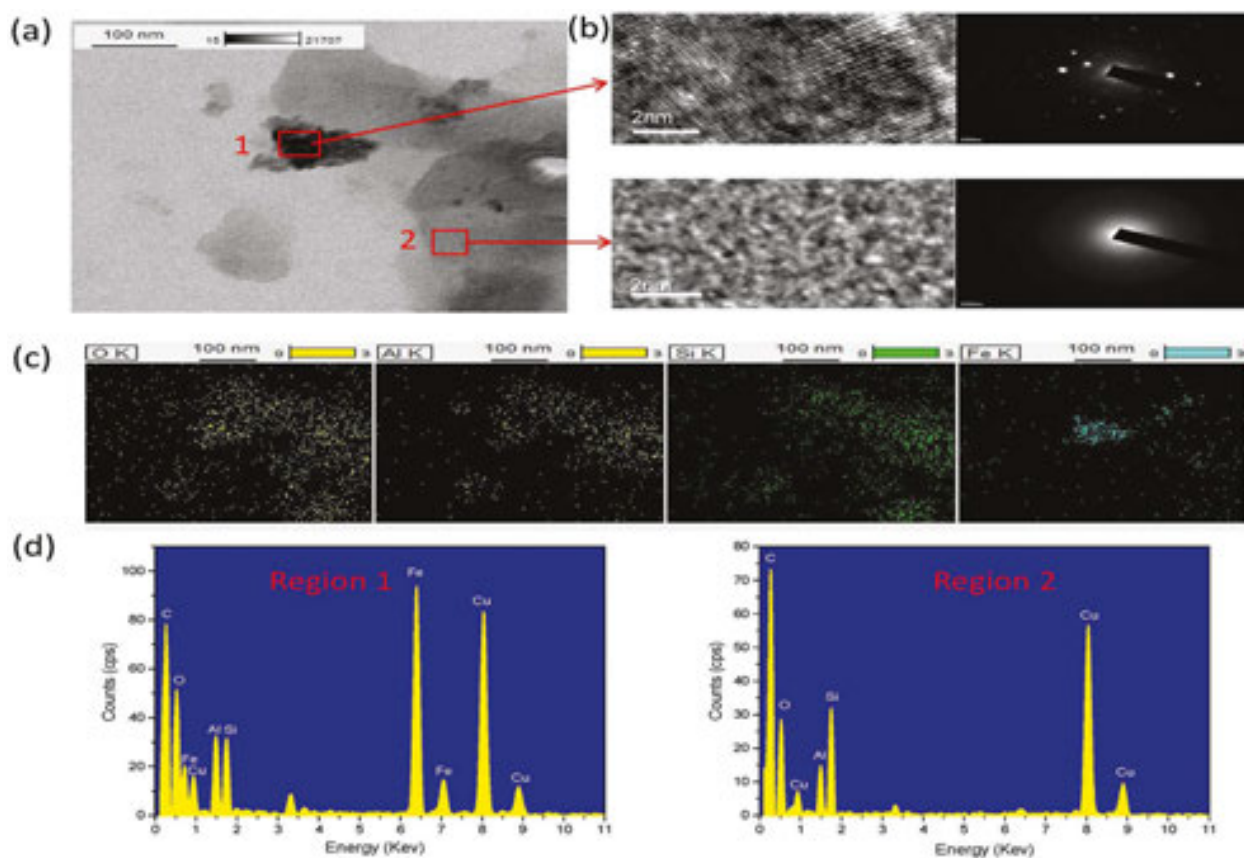


**Figure 11.** High-resolution transmission electron microscopy (HRTEM) images of soil dissolved organic matter from Control fertilization test in the long-term (22 years) location experiment. [4] (a) TEM image; (b) HRTEM images and selected area electron diffraction (SAED) pattern of the two regions indicated by blue squares, indicating that the black region is completely crystalline, while the gray region remains amorphous; (c) elemental maps; (d) EDS image. Control, no fertilization.
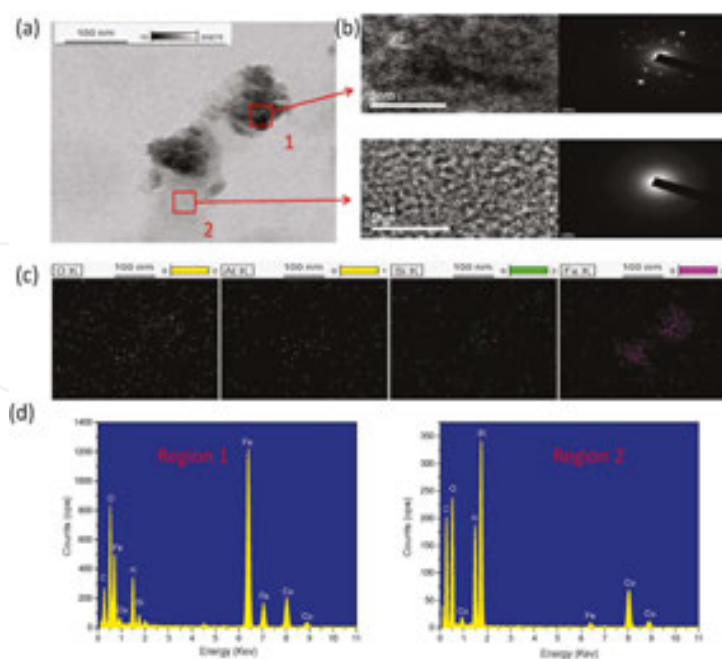
**Figure 12.** High-resolution transmission electron microscopy (HRTEM) images of soil-dissolved organic matter from NPK fertilization test in the long-term (22 years) location experiment. [4] (a) TEM image; (b) HRTEM images and selected area electron diffraction (SAED) pattern of the two regions indicated by blue squares, indicating that the black region is completely crystalline, while the gray region remains amorphous; (c) elemental maps; (d) EDS image. NPK, chemical nitrogen, phosphorus, and potassium fertilization.
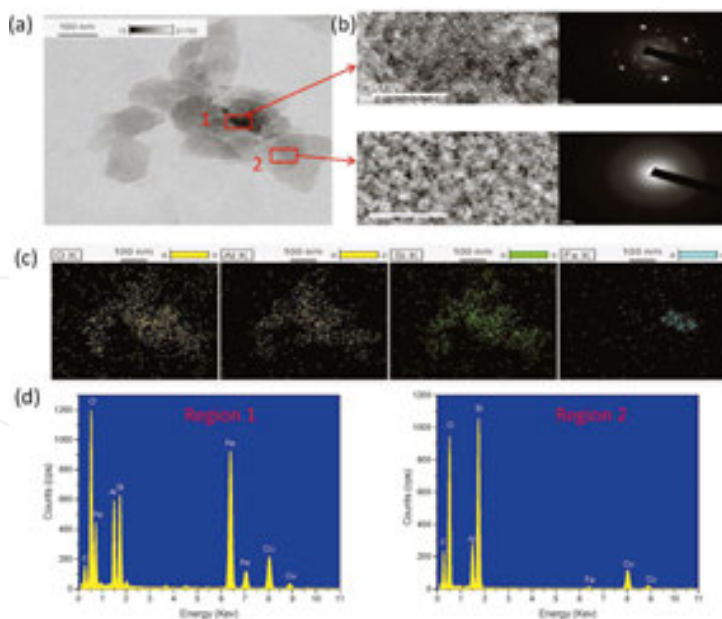


**Figure 13.** High-resolution transmission electron microscopy (HRTEM) images of soil-dissolved organic matter from NPKM fertilization test in the long-term (22 years) location experiment. [4] (a) TEM image; (b) HRTEM images and selected area electron diffraction (SAED) pattern of the two regions indicated by blue squares, indicating that the black region is completely crystalline, while the gray region remains amorphous; (c) elemental maps; (d) EDS image. NPKM, NPK plus manure fertilization.

To understand whether fertilization practices can affect the local coordination state and the environment of Al and Si, the [27]Al and [29]Si nuclear magnetic resonance spectroscopy (NMR) spectra of soil water-dispersible colloids were used (**Figure 14**). The results showed that octahedrally coordinated aluminum ([VI]Al), with a peak at approximately 0 ppm, was the only type of aluminum in the soil water-dispersible colloids under the 22-year long-term Control, M, and NPKM treatments (**Figure 14**). Although the octahedrally coordinated Al was also dominant in soil colloids under the NPK, NPKCa (NPK + lime), N, and NCa (N + lime), small amounts of distorted tetrahedrally coordinated aluminum ([IV]Al, 46 ppm) and pentahedrally coordinated aluminum ([V]Al, 25 ppm) were observed. Distorted [IV]Al and [V]Al are usually present in well-characterized crystalline minerals. [25–27] This finding strongly implies that chemical fertilization modified the local coordination state and environment of Al, with a small part of [IV]Al replaced by distorted [IV]Al and [V]Al, whereas organic fertilization or organic plus chemical fertilization did not influence the local coordination state and Al environment. The results from the high-resolution ^{27}Al NMR spectra support the finding that amorphous Al is more present in organic fertilizations (i.e., M and NPKM) than in chemical fertilizations (i.e., NPK, NPKCa, N, and NCa) (**Figure 15**). ^{29}Si NMR spectra also confirmed the presence of amorphous Al as allophane and imogolite in the soils under control, M, and NPKM, but not under the four chemical fertilizations (N, NCa, NPK, and NPKCa). These results from ^{27}Al and ^{29}Si NMR spectra are consistent with our previous publication, in which nanominerals were directly observed by HRTEM images of soil DOM. [4]
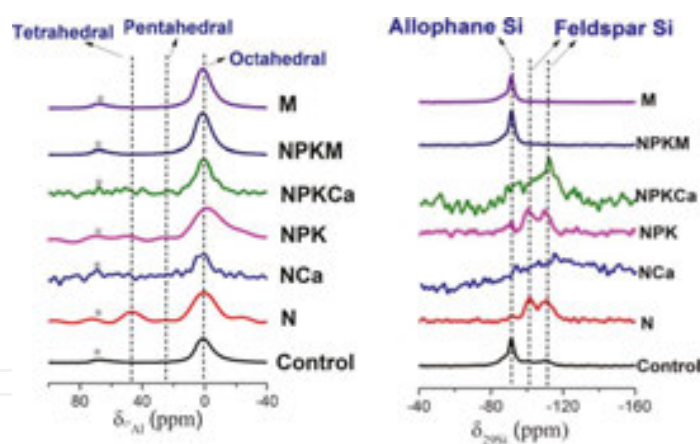


**Figure 14.** High-resolution ^{27}Al and ^{29}Si NMR spectra of water-dispersible colloids from the long-term fertilized soils. [28] Control, no fertilization; N, chemical nitrogen; NCa, chemical nitrogen plus lime; NPK, chemical nitrogen, phosphorus, and potassium; NPKCa, chemical nitrogen, phosphorus, and potassium plus lime; NPKM, NPK plus swine manure; and M, swine manure. The results of ^{29}Si NMR spectra support the presence of nanominerals in organic (i.e., NPKM and M) rather than chemical (i.e., N, NCa, NPK, and NPKCa) fertilization treatments.

Selective extraction also showed that the Al fractions were significantly ($P < 0.05$) altered by the long-term fertilization treatment (**Figure 10**). Significantly higher amorphous Al concentrations among the fertilizers were ranked as M ≈ NPKM > NPK ≈ NPKCa > N > NCa > Control (**Figure 10**). Significantly higher strongly organically bound Al concentrations ranked as NPKM > Control > NCa > NPK > NPKCa > M > N; significantly higher weakly organically

bound Al concentrations ranked as NCa ≈ NPKCa > NPKM ≈ NPK ≈ Control > M > N. In addition, significantly higher exchangeable Al concentrations ranked as N > NPK > NPKCa > NCa > Control > M ≈ NPKM. These four fractions followed the pattern: organically bound Al > amorphous Al fraction > exchangeable Al. The results demonstrated that organic fertilization treatments increased amorphous Al and reduced exchangeable Al compared with chemical fertilization treatments. The addition of lime significantly ($P < 0.05$) increased the weakly organically bound Al and reduced exchangeable Al, suggesting that lime amendment transferred Al fractions from exchangeable Al to the weakly organically bound Al. These trends definitely affected soil C sequestration and soil pH.
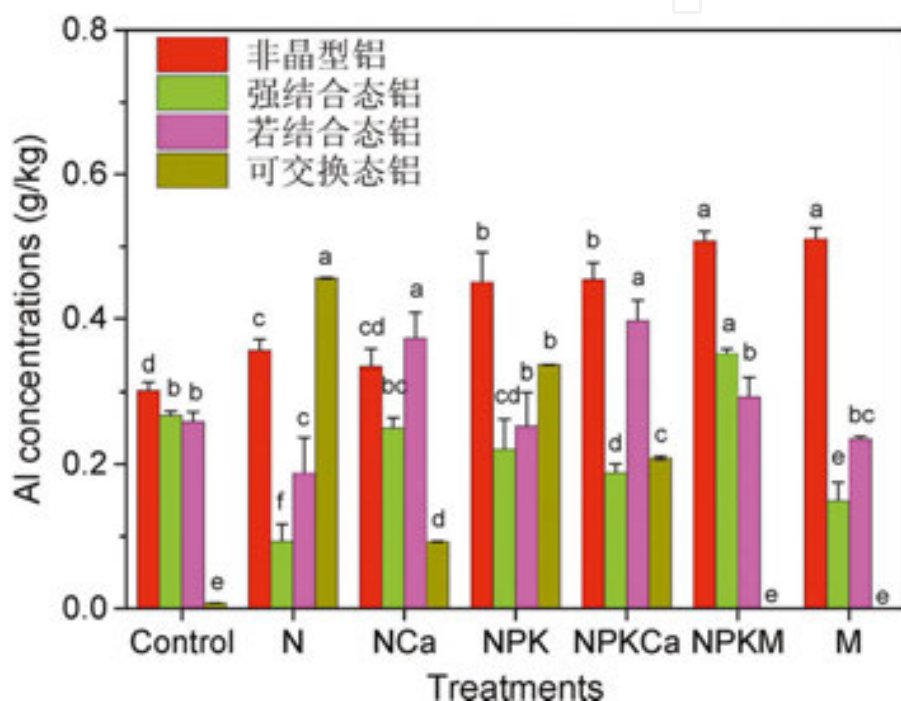


**Figure 15.** Aluminum fractions in the different fertilization treatments from the site of the long-term fertilization experiment, obtained by selective dissolution techniques. [28] Significant differences between fertilization treatments were determined using one-way ANOVA followed by Duncan's multiple range test at $P < 0.05$, in which conditions of normality and homogeneity of variance were met. The data are shown as mean ± SD ($n$ = 3). Control, no fertilization; N, chemical nitrogen; NCa, chemical nitrogen plus lime; NPK, chemical nitrogen, phosphorus, and potassium; NPKCa, chemical nitrogen, phosphorus, and potassium plus lime; NPKM, NPK plus swine manure; M, swine manure.

Meanwhile, Fe K-edge X-ray absorption fine structure spectroscopy (XAFS) is used for both identification and quantification of different mineral phases present in soil colloids.[5,29] Linear combination fitting (LCF) of soil colloids (**Figure 16** and **Table 6**) showed that goethite (56.8–67.0%) and hematite (14.9–25.0%) were prominent under all three fertilizations. The remaining Fe phases were composed of the less crystalline ferrihydrite species. The percentage of ferrihydrite was the highest under NPKM (18.0 ± 0.02%), followed by Control (16.0 ± 0.03%) and NPK (6.30 ± 0.02%). In view of the better C binding and potential preservation capability of ferrihydrite when compared to goethite and hematite,[5,30-32]. Fe minerals under organic fertilization should have a greater C loading than chemical fertilization.
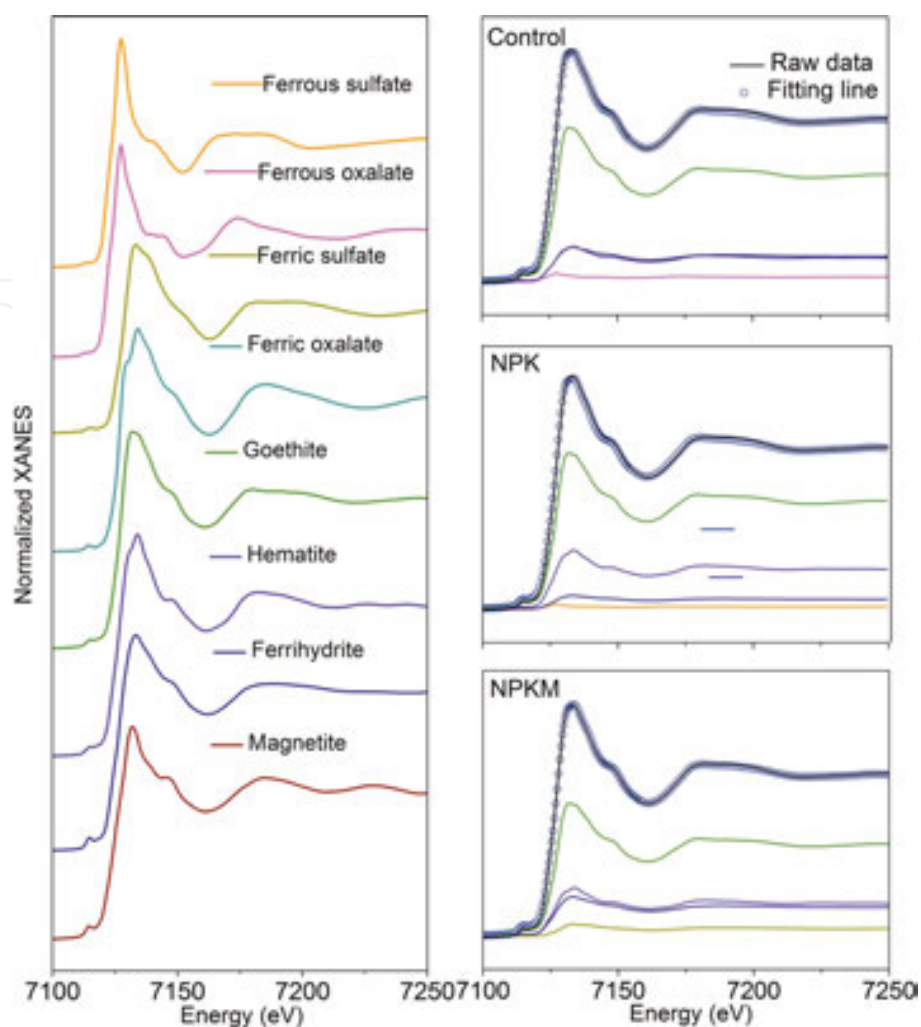
**Figure 16.** Fe K-edge XANES spectra of reference materials and soil colloids from three contrasting long-term (1990–2014) fertilization treatments. [29] The scattered circles represent the linear combination fitting (LCF) results of the sample spectra. Control, no fertilization; NPK, chemical nitrogen, phosphorus, and potassium fertilization; NPKM, chemical NPK plus swine manure fertilization.

| Treatment | LCF results (%) | | | | | | LCF parameters | |
|---|---|---|---|---|---|---|---|---|
| | Goethite | Hematite | Ferrihydrite | Ferric sulfates | Ferrous citrates | Ferrous sulfates | R-factor | Chi-square |
| **Control** | 66.0 ± 0.025 | 14.9 ± 0.000 | 16.0 ± 0.025 | ND | 3.10 ± 0.012 | ND | 0.000052 | 0.00437 |
| **NPK** | 67.0 ± 0.025 | 25.0 ± 0.000 | 6.30 ± 0.020 | ND | ND | 1.70 ± 0.008 | 0.000051 | 0.00426 |
| **NPKM** | 56.8 ± 0.025 | 20.4 ± 0.000 | 18.0 ± 0.017 | 4.8 ± 0.018 | ND | ND | 0.000051 | 0.00436 |

Note: Control, no fertilization; NPK, chemical nitrogen, phosphorus, and potassium fertilization; NPKM, chemical NPK plus swine manure fertilization; ND, not detected. Determination of parameters of fit (i.e., R-factor and Chi-square) indicated that the LCF results are convincing.

**Table 6.** Linear combination fit (LCF) results of Fe K-edge XANES spectra of the soil colloids from three separate long-term (1990–2014) fertilization treatments [29]

Nanoscale secondary ion mass spectrometry (NanoSIMS) has the potential to examine the spatial integrity of soil microenvironments and has been designed for high lateral resolution (down to 50 nm) imaging, while still maintaining high mass resolution and high sensitivity (mg kg$^{-1}$ range).[5,33]. NanoSIMS images, combined with the region of interests (ROIs) analysis, were used to explore the C-binding capability of Al and Fe minerals. Based on the pixel value of secondary $^{12}C^-$ ion mass in all spots from each sample, the selected ROIs were identified. The selected ROIs were further divided into $^{12}C^-$-rich and $^{12}C^-$ less-rich ROIs. The area percentage of the $^{12}C^-$-rich or $^{12}C^-$ less-rich ROIs accounted for 7.47 or 40.18%, 10.80 or 27.64%, and 8.23 or 37.99% under Control, NPK, and NPKM, respectively. Interestingly, the box plots (**Figure 17**) of $^{12}C^-/^{27}Al^{16}O^-$ (a, b) and $^{12}C^-/^{56}Fe^{16}O^-$ (c, d) ratios showed that both the median and the mean values were higher under NPKM than under NPK. These results suggest that Al and Fe minerals under NPKM can bind more organic C than those of NPK.
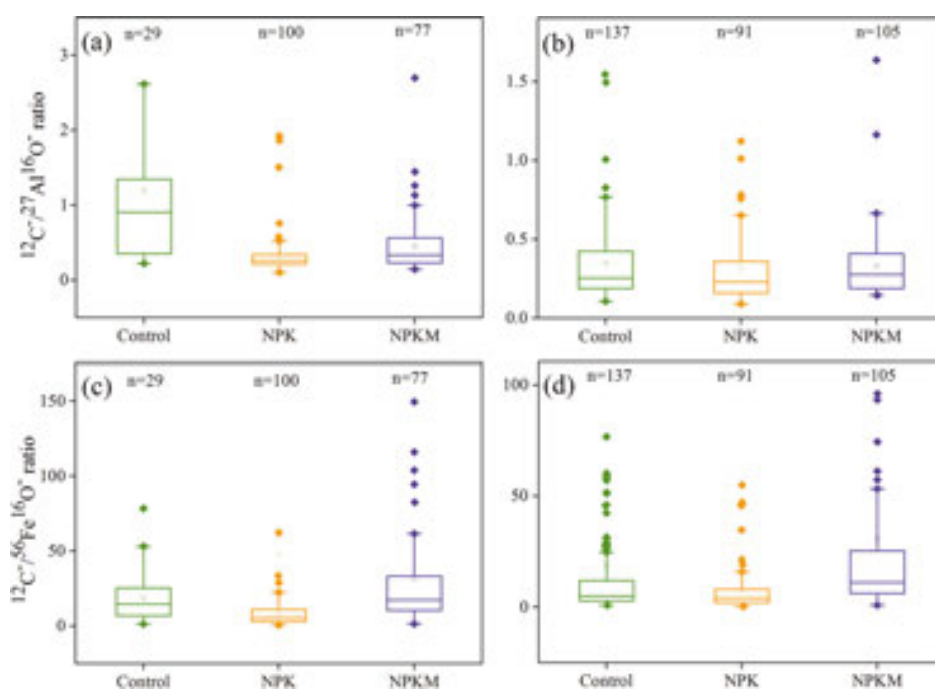


**Figure 17.** Box plots of $^{12}C^-/^{27}Al^{16}O^-$ (a, b) and $^{12}C^-/^{56}Fe^{16}O^-$ (c, d) ratios reflecting the $^{12}C^-$ rich ROIs (a, c) and $^{12}C^-$ less rich ROIs (b, d) of the soil colloids from three contrasting long-term (1990–2014) fertilization treatments using Nano-SIMS (for all spots). [29] Control, no fertilization; NPK, chemical nitrogen, phosphorus, and potassium fertilization; NPKM, chemical NPK plus swine manure fertilization. The $^{12}C^-$ rich ROIs include the areas above 90 pixels, and the $^{12}C^-$ less rich ROIs include the areas in the range of 90–40 pixels under Control and NPK, which were above 50 pixels, and in the range of 50–30 pixels under NPKM. The number $n$ in figures represents the number of the selected ROIs. The line in the middle of the box is the median value and the square in the box is the mean value. The lines that protrude out of the boxes represent the 25th and 75th population percentiles. Outliers are shown as diamonds.

To address the specific C components preserved by reactive minerals, synchrotron-based C 1s near-edge X-ray fine structure (NEXAFS) spectroscopy was used to identify C composition. Compared to NPK treatment, NPKM and M treatments markedly increased carboxylic groups (288.4–289.1 eV) from 24.2 to 33.2% and increased both the aromatic (283.0–286.1 eV) and phenolic (286.2–287.5 eV) groups by greater than 2.8-fold (**Figure 18** and **Table 7**). In conclu-

sion, organic fertilization treatments (NPKM and M) enhanced the retention of carboxylic and aromatic C by reactive minerals in soils.
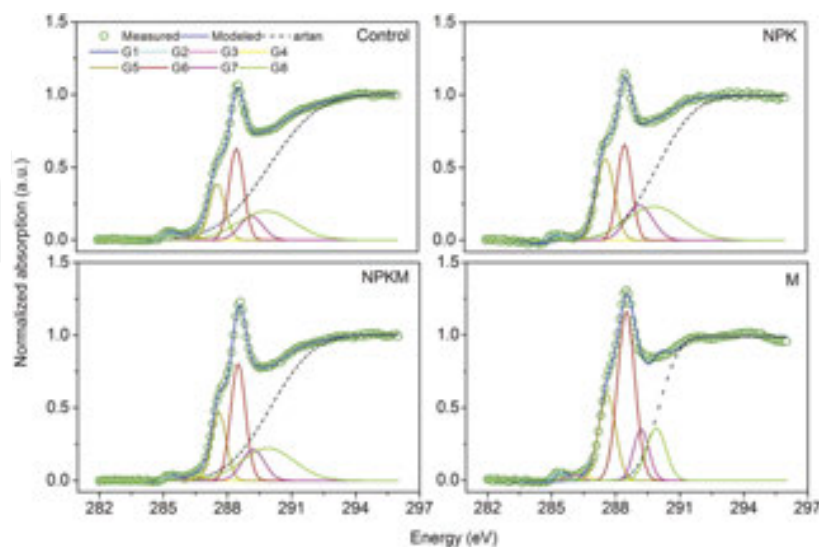


**Figure 18.** Organic C composition in the soil colloids from the various long-term fertilization treatments. [6] (a) Control, no fertilization; (b) NPK, chemical fertilization; (c) NPKM, chemical plus swine manure fertilization; (d) M, swine manure fertilization.

| Treatment | Proportion of absorption regions (%) | | | | | |
|---|---|---|---|---|---|---|
| | Aromatic C | Phenolic C | Alkyl C | Carboxylic C | O-alkyl C | Carbonyl C |
| | (283–286.1 eV) | (286.2–287.5 eV) | (287.6–288.3 eV) | (288.4–289.1 eV) | (289.2–289.8 eV) | (289.9–290.2 eV) |
| Control | 2.6 | 0.7 | 19.4 | 29.6 | 12.1 | 35.6 |
| NPK | 0.5 | 0.1 | 25.7 | 24.2 | 16.3 | 33.2 |
| NPKM | 1.4 | 1.1 | 18.9 | 33.2 | 13.2 | 32.2 |
| M | 1.8 | 0.5 | 22.9 | 46.6 | 12.3 | 15.9 |

Control, no fertilization; NPK, chemical fertilization; NPKM, chemical plus swine manure fertilization; M, swine manure fertilization.

**Table 7.** Deconvolution results for using C 1s NEXAFS on soil colloids from the various long-term fertilization treatments [6]

## 5. Conclusion

Composting is an inexpensive and sustainable treatment for solid organic wastes. The composting industry has been growing rapidly because of a boom in the animal industry in China over the past decades. In this chapter, we introduce composting process and status in China, especially in Jiangsu Province. Meanwhile, the developed novel spectroscopy techniques (i.e., NIRS-PLS and EEM-PARAFAC) are also introduced, which are more suitable for

assessment of compost maturity than the conventional techniques in view of ease of sample preparation, rapid spectrum acquisition, nondestructive nature of the analysis, and the portability of the technology. In addition, organic fertilizer amendments can not only improve soil fertility but also offset chemical fertilizers' nanoscale changes. Recently, investigators have shown that organic fertilizer amendments could enhance the production of highly reactive minerals, for example, allophane, imogolite, and ferrihydrite, which further benefit for soil carbon storage and soil fertility improvement.

## Acknowledgements

## Author details

Guanghui Yu*, Wei Ran and Qirong Shen

*Address all correspondence to: yuguanghui@njau.edu.cn

National Engineering Research Center for Organic-based Fertilizers, Jiangsu Provincial Key Lab for Organic Solid Waste Utilization, Jiangsu Collaborative Innovation Center for Solid Organic Waste Resource Utilization, Nanjing Agricultural University, Nanjing, PR China

## References

[1] Yu G.H. *et al*. PARAFAC modeling of fluorescence excitation-emission spectra for rapid assessment of compost maturity. *Bioresource Technology* 101, 8244–8251 (2010).

[2] Said-Pullicino D., Erriquens F.G. & Gigliotti G. Changes in the chemical characteristics of water-extractable organic matter during composting and their influence on compost stability and maturity. *Bioresource Technology* 98, 1822–1831 (2007).

[3]  Chadwick D. *et al*. Improving manure nutrient management towards sustainable agricultural intensification in China. *Agriculture, Ecosystems & Environment* 209, 34–46 (2015).

[4]  Wen Y. *et al*. Insights into complexation of dissolved organic matter and Al(III) and nanominerals formation in soils under contrasting fertilizations using two-dimensional correlation spectroscopy and high resolution-transmission electron microscopy techniques. *Chemosphere* 111, 441–449 (2014).

[5]  Xiao J. *et al*. In situ visualisation and characterisation of the capacity of highly reactive minerals to preserve soil organic matter (SOM) in colloids at submicron scale. *Chemosphere* 138, 225–232 (2015).

[6]  Huang C. *et al*. Spectroscopic evidence of the improvement of reactive iron mineral content in red soil by long-term application of swine manure. *PloS One* 11, e0146364 (2016).

[7]  Guo J.H. *et al*. Significant acidification in major Chinese croplands. *Science* 327, 1008–1010 (2010).

[8]  Tang Z., Yu G., Liu D., Xu D. & Shen Q. Different analysis techniques for fluorescence excitation-emission matrix spectroscopy to assess compost maturity. *Chemosphere* 82, 1202–1208 (2011).

[9]  Bernal M.P., Alburquerque J.A. & Moral R. Composting of animal manures and chemical criteria for compost maturity assessment. A review. *Bioresource Technology* 100, 5444–5453 (2009).

[10]  Wang C. *et al*. Rapid and accurate evaluation of the quality of commercial organic fertilizers using near infrared spectroscopy. *PloS One* 9, e88279 (2014).

[11]  Albrecht R., Joffre R., Petit J.L., Terrom G. & Périssol, C. Calibration of chemical and biological changes in cocomposting of biowastes using near-infrared spectroscopy. *Environmental Science & Technology* 43, 804–811 (2009).

[12]  Malley D.F., McClure C., Martin P.D., Buckley K. & McCaughey W.P. Compositional analysis of cattle manure during composting using a field-portable near-infrared spectrometer. *Communications in Soil Science and Plant Analysis* 36, 455–475 (2005).

[13]  Xing L., Chen L.J. & Han L.J. Rapid analysis of layer manure using near-infrared reflectance spectroscopy. *Poultry Science* 87, 1281–1286 (2008).

[14]  Albrecht R. *et al*. Efficiency of near-infrared reflectance spectroscopy to assess and predict the stage of transformation of organic matter in the composting process. *Bioresource Technology* 99, 448–455 (2008).

[15]  Henderson R.K. *et al*. Fluorescence as a potential monitoring tool for recycled water systems: A review. *Water Research* 43, 863–881 (2009).

[16] Plaza C., Senesi N., Brunetti G. & Mondelli D. Evolution of the fulvic acid fractions during co-composting of olive oil mill wastewater sludge and tree cuttings. *Bioresource Technology* 98, 1964–1971 (2007).

[17] Chen W., Westerhoff P., Leenheer J.A. & Booksh K. Fluorescence excitation–emission matrix regional integration to quantify spectra for dissolved organic matter. *Environmental Science & Technology* 37, 5701–5710 (2003).

[18] Yu G.H., He P.J. & Shao L.M. Novel insights into sludge dewaterability by fluorescence excitation-emission matrix combined with parallel factor analysis. *Water Research* 44, 797–806 (2010).

[19] Marhuenda-Egea F.C. *et al*. Dissolved organic matter fractions formed during composting of winery and distillery residues: Evaluation of the process by fluorescence excitation–emission matrix. *Chemosphere* 68, 301–309 (2007).

[20] Senesi N., Plaza C., Brunetti G. & Polo A. A comparative survey of recent results on humic-like fractions in organic amendments and effects on native soil humic substances. *Soil Biology and Biochemistry* 39, 1244–1262 (2007).

[21] Su Y.-Z., Wang F., Suo D.-R., Zhang Z.-H. & Du M.-W. Long-term effect of fertilizer and manure application on soil-carbon sequestration and soil fertility under the wheat–wheat–maize cropping system in northwest China. *Nutrient Cycling in Agroecosystems* 75, 285–295 (2006).

[22] Maillard E. & Angers D.A. Animal manure application and soil organic carbon stocks: a meta-analysis. *Global Change Biology* 20, 666–679 (2014).

[23] Liu H. *et al*. Mitigating greenhouse gas emissions through replacement of chemical fertilizer with organic manure in a temperate farmland. *Science Bulletin* 60, 598–606 (2015).

[24] Zhou H., Peng X., Perfect E., Xiao T. & Peng G. Effects of organic and inorganic fertilization on soil aggregation in an Ultisol as characterized by synchrotron based X-ray micro-computed tomography. *Geoderma* 195–196, 23–30 (2013).

[25] Hiradate S. & Wada S.-I. Weathering process of volcanic glass to allophane determined by 27Al and 29Si solid-state NMR. *Clays and Clay Minerals* 53, 401–408 (2005).

[26] Kang D.-Y. *et al*. Dehydration, dehydroxylation, and rehydroxylation of single-walled aluminosilicate nanotubes. *ACS Nano* 4, 4897–4907 (2010).

[27] Kindler R. *et al*. Dissolved carbon leaching from soil is a crucial component of the net ecosystem carbon balance. *Global Change Biology* 17, 1167–1185 (2011).

[28] Wen Y.L. *et al*. Long-term fertilization practices alter aluminum fractions and coordinate state in soil colloids. *Soil Science Society of America Journal* 78, 2083–2089 (2014).

[29] Xiao J. *et al*. In situ interactive characteristics of reactive minerals in soil colloids and soil carbon preservation differentially revealed by nanoscale secondary ion mass

spectrometry and X-ray absorption fine structure spectroscopy. *Biogeosciences Discussion* 2016, 1–39 (2016).

[30] Baker, L.L., Strawn, D.G., Vaughan, K.L. & McDaniel, P.A. XAS Study of Fe Mineralogy in a Chronosequence of Soil Clays Formed in Basaltic Cinders. *Clays and Clay Minerals* 58, 772-782 (2010).

[31] Kramer, M.G., Sanderman, J., Chadwick, O.A., Chorover, J. & Vitousek, P.M. Long-term carbon storage through retention of dissolved aromatic acids by reactive particles in soil. *Global Change Biology* 18, 2594-2605 (2012).

[32] Lalonde, K., Mucci, A., Ouellet, A. & Gelinas, Y. Preservation of organic matter in sediments promoted by iron. *Nature* 483, 198-200 (2012).

[33] Herrmann, A.M. et al. Nano-scale secondary ion mass spectrometry — A new analytical tool in biogeochemistry and soil ecology: A review article. *Soil Biology and Biochemistry* 39, 1835-1850 (2007).